CONSTITUTIVE EQUATION WITH INTERNAL DAMPING FOR MATERIALS UNDER CYCLIC AND DYNAMIC LOADINGS IN THE FRAMEWORK OF SMALL STRAIN ELASTOPLASTICITY

Ladislav ÉCSI[1] – Pavel ÉLESZTŐS[1]

[1] Institut of Apllied Mechanics and Mechatronics, Faculty of Mechanical Engineering, Slovak University of Technology in Bratislava, ladislav.ecsi@stuba.sk

ABSTRACT

In this paper a universal constitutive equation with internal damping [1] is presented for materials under dynamic and cyclic loadings. The model adapts the idea of a spring dashpot system connected in parallel for continuum, utilizing appropriate deformation measures, which are independent of rigid body motion thus enabling more precise numerical simulation of a deformable body. In the presented work the model application is shown in numerical examples using cyclic tension of a prismatic bar and free vibration of a cantilever beam. The examples were solved within the framework of small strain elastoplasticity [2], employing the extended NoIHKH material model for cyclic plasticity of metals [3], [4].

Keywords: finite element method, small strain elastoplasticity, cyclic plasticity of metals, internal damping

INTRODUCTION

An engineering construction, during its period of operation, has to withstand various loadings, the majority of which can be characterized as dynamic or cyclic. To properly model the behaviour of such constructions internal damping of their material has to be taken into account. In contemporary computational mechanics the Rayleigh damping [5] model is used exclusively to model energy dissipations originating from material damping. The major disadvantage of the model is that it does not differentiate between rigid body motion and deformation. Recently a new, universal constitutive equation with internal damping was proposed [1] to solve the aforementioned problem. The model adapts the idea of a spring dashpot system connected in parallel for continuum, utilizing appropriate deformation measures, which are independent of rigid body motion, thus enabling more precise numerical simulation of a deformable body.

THEORETICAL BACKGROUND

The conservation of linear momentum of a solid deformable body of volume Ω and surface $\partial\Omega$, idealized as non-polar continuum can be written in the following variational form

$$\int_{\Omega} \rho \dot{\mathbf{v}} \cdot \delta \mathbf{v} dv + \int_{\Omega} \boldsymbol{\sigma} : \delta \mathbf{d} dv = \int_{\Omega} \mathbf{b} \cdot \delta \mathbf{v} dv + \int_{\partial\Omega} \mathbf{t} \cdot \delta \mathbf{v} ds. \qquad (1)$$

In equation (1) $\rho, \mathbf{v}, \boldsymbol{\sigma}, \mathbf{d}, \mathbf{b}, \mathbf{t}$ denote the material density, the velocity vector, the Cauchy stress tensor, the strain rate tensor, the body force and the surface traction vector at a material point of the body. Considering the analogy between continuum and a spring dashpot system connected in parallel, where the spring force/damping force depends on the relative displacement/relative velocity of the spring ends, the Cauchy stress tensor of a material with internal damping can be expressed within the framework of small strain elastoplasticity [2] , [6] in the following incremental form

$$ {}^{n+1}\boldsymbol{\sigma} = {}^{n+1}\boldsymbol{\sigma}^{el} + {}^{n+1}\boldsymbol{\sigma}^{damp}, \tag{2} $$

where

$$ {}^{n+1}\boldsymbol{\sigma}^{el} = \Delta\boldsymbol{\sigma}^{el} + {}^{n}\boldsymbol{\sigma}^{el}, \tag{3} $$

$$ \Delta\boldsymbol{\sigma}^{el} = \Delta t\mathrm{C} : {}^{n+\frac{1}{2}}\mathbf{d}, \text{ in elastic loading / unloading} \tag{4} $$

$$ \Delta\boldsymbol{\sigma}^{el} = \Delta t\mathrm{C} : \left({}^{n+\frac{1}{2}}\mathbf{d} - {}^{n+\frac{1}{2}}\mathbf{d}^{pl} \right), \text{ in plastic loading} \tag{5} $$

$$ {}^{n+1}\boldsymbol{\sigma}^{damp} = \mathrm{C}^{damp} : {}^{n+1}\mathbf{d}, \tag{6} $$

$$ \mathrm{C} = 2G\mathrm{I} + \lambda\left(\mathbf{1}\otimes\mathbf{1}\right),\ G = \frac{E}{2\left(1+\nu\right)},\ \lambda = \frac{\nu E}{\left(1+\nu\right)\left(1-2\nu\right)}, \tag{7} $$

$$ \mathrm{C}^{damp} = 2G^{damp}\mathrm{I} + \lambda^{damp}\left(\mathbf{1}\otimes\mathbf{1}\right),\ G^{damp} = \frac{E^{damp}}{2\left(1+\nu^{damp}\right)},\ \lambda^{damp} = \frac{\nu^{damp}E^{damp}}{\left(1+\nu^{damp}\right)\left(1-2\nu^{damp}\right)}, \tag{8} $$

Equation (3) determines the elastic part of the Cauchy stress tensor(2), and equation (6) defines its damping part. In the elastic Cauchy stress update calculation the conventional small strain elastoplasticity theory was used, where the elastic Cauchy stress increment is either expressed with formula (4) in elastic loading and unloading, or with formula (5) in plastic loading. Here the left superscripts $n, n+1/2, n+1$ denote the variable value at discrete times corresponding to previous, mid and current configurations of the body within the current time step Δt. We assume that the material is isotropic, and that the strain rate tensor has the additive decomposition $\mathbf{d} = \mathbf{d}^{el} + \mathbf{d}^{pl}$ into an elastic part $\mathbf{d}^{el}$ and a plastic part $\mathbf{d}^{pl}$. In this work the St. Venant-Kirchov material is used, the elastic material tensor C of which can be expressed with formula(7). In equation (7) G and λ denote the shear modulus and the Lame's constant, $\mathrm{I}, \mathbf{1}$ stand for a fourth-order unit tensor and a second-order unit tensor respectively and ν, E are the Poisson ratio and the Young modulus. The fourth-order damping tensor C^{damp} is formally constructed in the same way, equation (8) as the elastic material tensor using two independent variables ν^{damp}, E^{damp}, which ensures isotropy.
Equations (1)-(6) are supplemented with the following constitutive and evolution equations:

$$ f = \sigma_{eq} - \sigma_y - R \le 0, \tag{9} $$

$$ \sigma_{eq} = \sqrt{\frac{3}{2}\left(\boldsymbol{\Sigma}-\mathbf{X}\right) : \left(\boldsymbol{\Sigma}-\mathbf{X}\right)}, \tag{10} $$

$$ R = Q\left(1 - e^{-b\varepsilon^{pl}}\right), \tag{11} $$

$$ \dot{\mathbf{X}} = \mathrm{C}^{cycl} : \mathbf{d}^{pl} - \gamma\left(\varepsilon^{pl}\right)\mathbf{X}\dot{\varepsilon}^{pl};\quad tr\left(\mathbf{X}\right) = 0, \tag{12} $$

$$ \gamma\left(\varepsilon^{pl}\right) = \gamma_\infty - \left(\gamma_\infty - \gamma_0\right)e^{\left(-\omega\varepsilon^{pl}\right)}, \tag{13} $$

$$ \mathrm{C}^{cycl} = 2G^{cycl}\mathrm{I} + \lambda^{cycl}\left(\mathbf{1}\otimes\mathbf{1}\right),\ G^{cycl} = \frac{E^{cycl}}{2\left(1+\nu^{cycl}\right)},\ \lambda^{cycl} = \frac{\nu^{cycl}E^{cycl}}{\left(1+\nu^{cycl}\right)\left(1-2\nu^{cycl}\right)}. \tag{14} $$

Equations (9)-(14) represent the extended NoIHKH material model for cyclic plasticity of metals [3] based on the NoIHKH material model [4]. The model uses combined isotropic and kinematic hardening and employs associative plasticity in the elastic-plastic material tensor derivation.

Equation (9) defines the yield surface and formulas (11) and(12) define the NoIH rule for isotropic hardening and the NoKH rule for kinematic hardening. Here $\boldsymbol{\Sigma}, \mathbf{X}, \varepsilon^p, \dot{\varepsilon}^p$ stand for the deviatoric component of the Cauchy stress tensor, a back stress tensor, an accumulated plastic strain and an accumulated plastic strain rate. The remaining symbols denote constant material parameters. The fourth-order cyclic material tensor $\mathbf{C}^{cyc}$ is formally constructed in the same way (14) as the elastic material tensor using two independent variables E^{cyc}, ν^{cyc}, which ensure isotropy.

NUMERICAL EXAMPLE NO. 1 – CYCLIC TENSION OF A PRISMATIC BAR

As a numerical example a prismatic bar of $1\,\mathrm{m} \times 1\,\mathrm{m} \times 3\,\mathrm{m}$ was studied, applying cyclic tension. One end of the bar was fixed and the second end underwent a prescribed axial deformation determined by a sine function and an amplitude of $2.5 / 3.5\,\mathrm{mm}$ corresponding to elastic/elastic-plastic loading case, while it was guided in the remaining two directions. In the numerical experiment one loading cycle was realized using 15 degree angular increments in each time step. Cases with and without internal dampings were studied, using $0.04\,Hz$, $4.16\,Hz$ and $41.66\,Hz$ loading frequency, corresponding to $1.0\,s$, $0.01\,s$ and $0.001\,s$ time step values. The numerical simulations were run as transient static ones using implicit time integration. As a simplification, all material properties were considered to be constant. Table 1 contains the used material parameters.

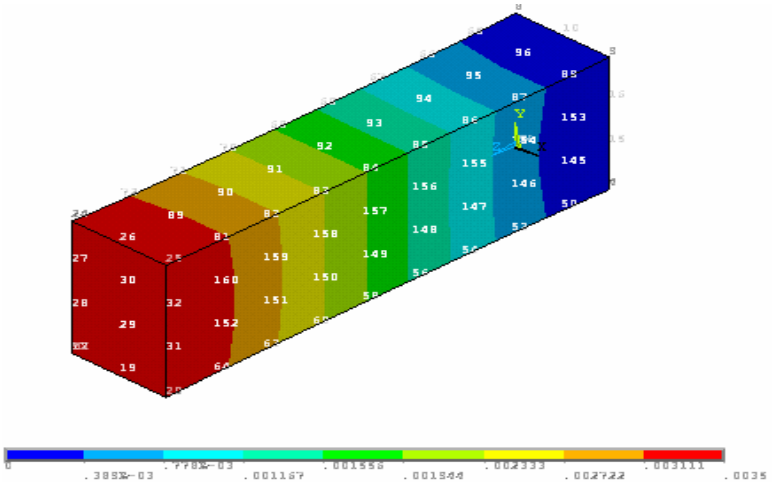

Fig. 1 Maximum axial deformation in one longitudinal cross section of the bar in elastic-plastic loading case.

Tab. 1 Material properties of the prismatic bar.

E [Pa]	E^{cycl} [Pa]	E^{damp} [Pa · s]	$\nu = \nu^{cycl} = \nu^{damp}$ [-]	σ_y [Pa]
$2.1 \cdot 10^{11}$	$2.1 \cdot 10^{5}$	$0.0 / 2.1 \cdot 10^{8}$	0.3	$2.0 \cdot 10^{8}$
Q [Pa]	b [-]	γ_∞ [-]	γ_0 [-]	ω [-]
$5.0 \cdot 10^{7}$	3.0	20.0	10.0	10.0

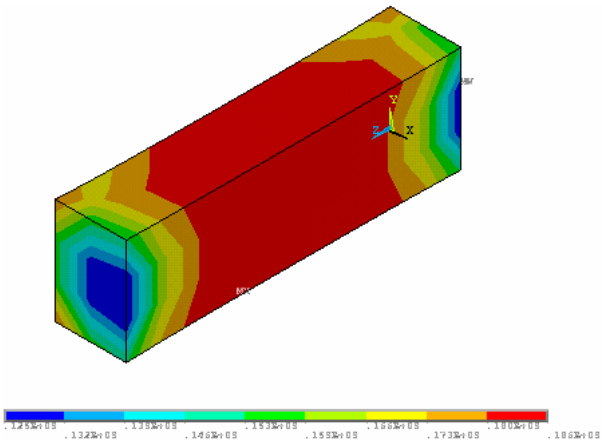

Fig. 2 Von Mises stress in one longitudinal cross section of the bar in elastic-plastic loading case.

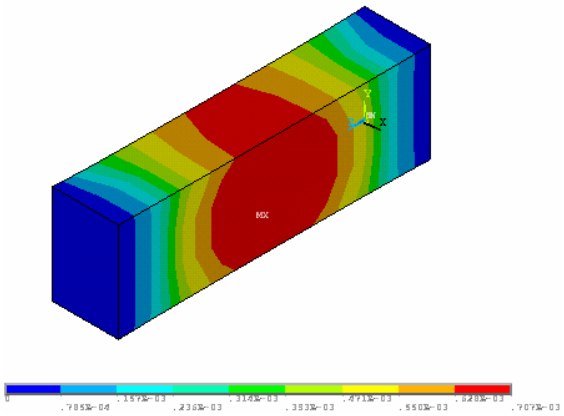

Fig. 3 Accumulated plastic strain in one longitudinal cross section of the bar in elastic-plastic loading case.

Figures 1-3 show the axial deformation, Von Mises stress and the accumulated plastic strain distribution in one longitudinal cross section of the bar at maximum tension corresponding to the elastic-plastic loading case with internal damping and 41.66 *Hz* loading frequency.
Figures 4-5 show the axial deformation versus axial stress curves at selected nodes at the bar end N30, and in its middle part at node N149 (See fig. 1 for the exact location of the nodes) corresponding to elastic/elastic-plastic loading. As can be seen in figure 4, there was no energy dissipation in elastic loading cases without damping, the system remained conservative and the axial deformation versus axial stress curve was linear. When internal damping hysteresis loops were applied, the material curve was no longer linear. Figures 4 and 5 imply that the area of the hysteresis loop is proportional to the deformation rate, i.e. the higher the deformation rate the greater the loop area as well as the amount of dissipated energy. Also, in limiting state, as the deformation rate approaches zero, the effect of internal damping vanishes.

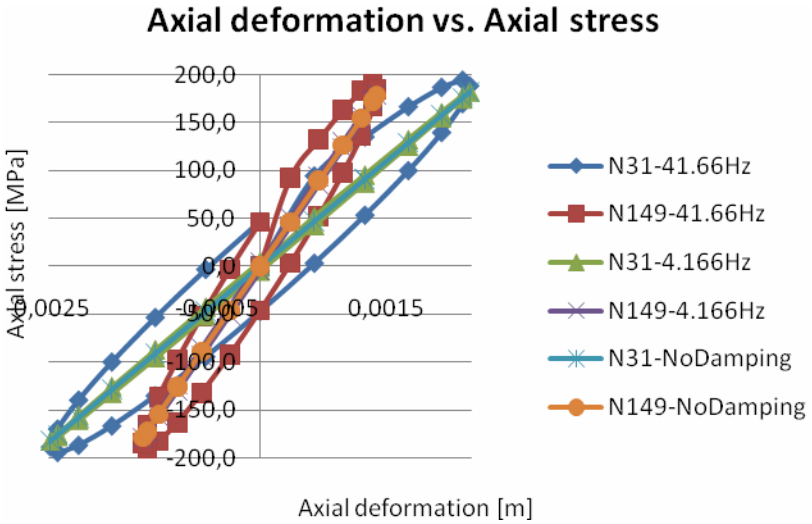

Fig. 4 Hysteresis loops at nodes N31, N149 using elastic loading.

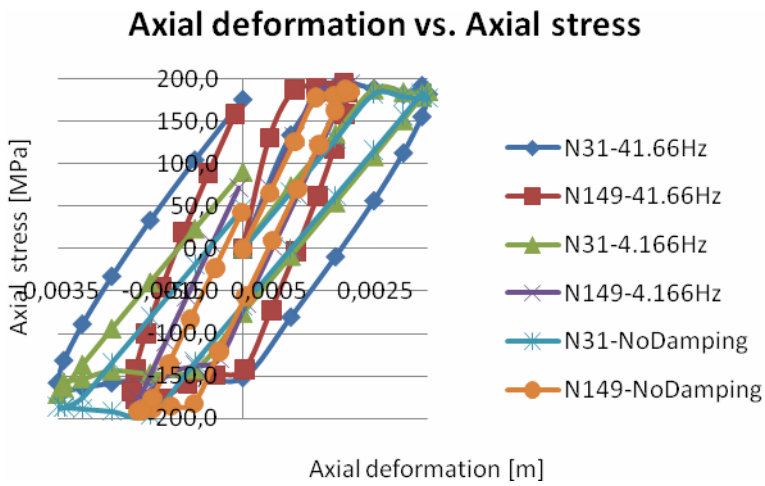

Fig. 5 Hysteresis loops at nodes N31, N149 using elastic-plastic loading.

NUMERICAL EXAMPLE NO. 2 – FREE VIBRATION OF A CANTILEVER BEAM

As a second numerical example a cantilever beam of length 12m and rectangular cross section, size 1m x 1m was studied. One end of the beam was fixed and the second end was loaded dynamically, applying a stepped load at its free end as pressure between 0.0 and1.0 MPa . The loading was determined in such way that no plastic deformations took place in the material of the

body. Figure 6 depicts the beam geometry, the boundary conditions and the applied pressure at the beam fee end as red arrows.

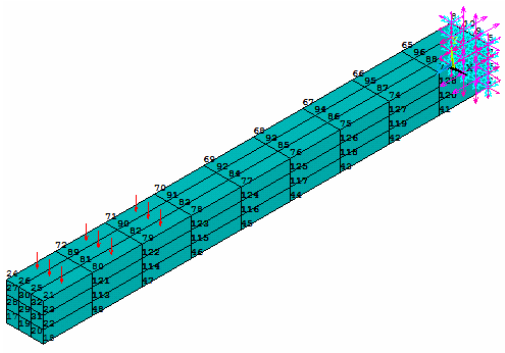

Fig. 6 Geometry of the cantilever beam.

In the numerical example free vibration with/without internal damping of the cantilever beam was studied using implicit dynamic analysis and constant, $\Delta t = 0.01$ s time step size. Table 2 lists the material properties of the beam.

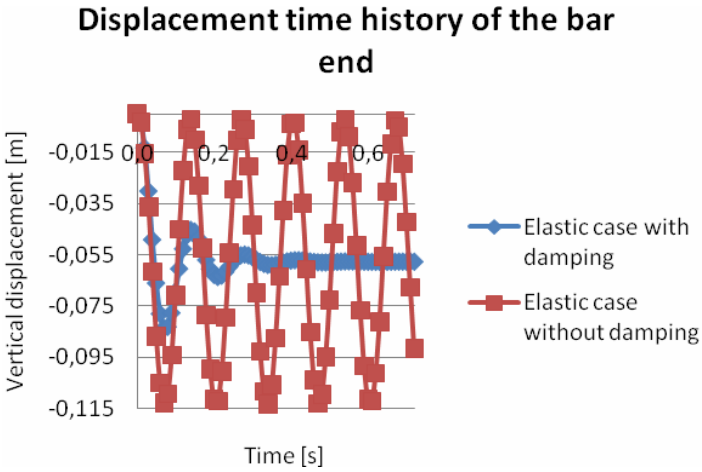

Fig. **7** Vertical displacement time history of the bar free end.

Table 2 Material properties of the cantilever beam.

ρ [kg · m^{-3}]	7800.0
E [GPa]	210.0
E^{damp} [GPa]	2.1/0.0
ν [-]	0.3
ν^{damp} [-]	0.3

Figure 7 shows the vertical displacement time history of the free end of the cantilever beam. As can be seen, mechanical energy dissipation took place if internal damping was applied, resulting in the beam ~~to~~ reaching the static equilibrium after a few cycles. On the other hand the system remained conservative without mechanical energy dissipation if no internal damping was applied.

CONCLUSION

In this paper a universal constitutive equation with internal damping for cyclically and dynamically loaded deformable bodies using small strain elastoplasticity was presented. Cyclic tension of a prismatic bar and free vibration of a cantilever beam was studied. The presented mathematical model is the only one in contemporary computational mechanics that can simulate the true energy dissipations originating from internal damping. As the model is independent of rigid body motion, it significantly improves the accuracy of the analyses. This applies in particular to problems with high deformation rates.

ACKNOWLEDGEMENT

Funding using VEGA grant 1/0488/09 and 1/0051/10 resources is greatly appreciated.

REFERENCES

[1] ÉCSI, L. - ÉLESZTŐS, P. 2008. Constitutive equation with internal damping for materials under dynamic and cyclic loadings, Proc. of the 46th International conference in experimental stress analysis 2008, EAN 2008, Horní Bečva, ČR, pp. 51-54.

[2] SIMO, J. C. - HUGHES, T. J. R. 1998. Computational inelasticity, Springer, NY.

[3] ÉCSI, L. 2006. Extended NoIHKH model usage for cyclic plasticity of metals, Engineering Mechanics, Vol. 13, Nr. 2, pp. 83-92.

[4] LEMAITRE, J. 2001. Handbook of material behaviour models, Deformations of materials, Vol. 1, Academic press, London.

[5] SUN, C. T., LU, Y.P. 1995. Vibration damping of structural elements, Prentice Hall PTR., Englewood Cliffs, New Jersey.

[6] MARDSEN, J. E. - HUGHES, T. J. R. 1983: Mathematical foundations of elasticity, Prentice-Hall, Inc, Englewood Cliffs, New Jersey.